# A Testbed for Evaluating LTE in High-Speed Trains

José Rodríguez-Piñeiro, José A. García-Naya, Ángel Carro-Lagoa and Luis Castedo
Department of Electronics and Systems, University of A Coruña, Spain
Email: {j.rpineiro, jagarcia, acarro, luis}@udc.es

***Abstract*—Long Term Evolution (LTE) is expected to substitute Global System for Mobile Communications as the basis technology for railway communications. Recently, special attention has been deserved to High-Speed Trains (HSTs) as this particular environment (mainly due to the high speed condition) can severely impact wireless systems performance. Although several channel models have been derived during the few last years, most of them are not accurate enough as they are not supported by measurement campaigns. In this paper, the main requirements for HST environments are analyzed and a flexible, cost-affordable, and easily-scalable software and hardware architecture for a testbed suitable for assessing LTE at high speeds is proposed.**

***Keywords*—LTE, railway, testbed, measurement campaigns.**

## I. Introduction

Nowadays, the most widely used communication system between trains and the elements involved in operation, control, and intercommunication of the railway infrastructure is based on adapting the Global System for Mobile Communications (GSM) technology, namely GSM for Railways (GSM-R). The performance of GSM-R is not adequate for supporting advanced services such as automatic pilot applications for trains or provisioning broadband services to the train staff and passengers. Moreover, maintenance costs are increasing because GSM-R devices are ad-hoc solutions based on legacy technology. At the same time, the increasing number of broadband services available for mobile devices motivated the migration from third-generation mobile networks to the fourth generation ones, being Long Term Evolution (LTE) the mainly adopted technology. Therefore, LTE is a good candidate to substitute GSM as the basis technology for railways. On the other hand, the introduction of high-speed trains attracted new users and provided a wide range of new possibilities.

One of the most important challenges dealing with the design of any wireless transmission technique is the accurate characterization of the channel model, specifically those involving movement of TX and/or RX nodes. In fact, channel model characterization can have implications on several aspects of the communications system design and test, such as network planning or synchronization techniques.

**Main Contributions** The main contributions of this paper are the formal establishment of the measurement requirements for High-Speed Train (HST) environments as well as the description of a complete hardware and software architecture suited to be used as a testbed in such environments.

## II. State of the Art and Motivation

In the last few years, several radio channel models were proposed based on measurement campaigns in different environments [1], such as those developed by the research projects COST207[1] (development of Second Generation of Mobile Communications – GSM) [2], COST231 (GSM extension and Third Generation systems) [3], COST259 [4] and COST273 [5], which form the basis of International Telecommunication Union (ITU) standards for channel models of Beyond 3G systems. Code Division Testbed (CODIT) [6] and Advanced TDMA Mobile Access (ATDMA) [7] focus on wideband channel modeling, specifically for Third Generation systems.

The ITU channel models [8] were used at the development of the Third Generation radio access systems. Although they include a vehicular radio environment, no high-speed propagation conditions are explicitly considered. The ITU channel models were also the basis for the specification of propagation conditions in the 3rd Generation Partnership Project (3GPP) specifications for Universal Mobile Telecommunications System (UMTS) [9]. In fact, the HST environment was first proposed by Siemens in 2005 [10]. The increase in bandwidth of LTE techniques compared to UMTS motivated the definition of Extended ITU models. Thus, the 20 MHz LTE channel models were defined based on previous existing models such as the ITU and 3GPP models [11]. Three values for the Doppler shift were considered, which correspond to three different mobile speeds given the carrier frequency. It is worth noting that LTE conformance tests also include propagation conditions for two HST scenarios for non-fading propagation channels, with speeds of 300 and 350 km/h, respectively [12]. It must be stated that the aforementioned HST scenarios are mainly focused on the impact of the Doppler Frequency for a specified network deployment while other channel characteristics are omitted.

In order to allow the evaluation of Multiple-Input, Multiple-Output (MIMO) schemes for High Speed Downlink Packet Access (HSDPA), 3GPP and 3rd Generation Partnership Project 2 (3GPP2) developed a geometry-based stochastic channel model, namely Spatial Channel Model (SCM) [13], which was later extended under the name of SCM-Extension (SCME) by the IST-WINNER project [14], increasing the channel bandwidth up to 100 MHz. A simplified version of SCME channel models was used in LTE design [15]. Additionally, WINNER radio channel models were developed. The so-called Phase II model [16] covers the frequency range from 2 to 6 GHz. It defines 13 propagation scenarios, including moving networks.

In 2008, the ITU Radiocommunication Sector (ITU-R) approved radio channel models for the evaluation of IMT-Advanced technologies, like LTE-Advanced (LTE-A) [17], [18], partially based on WINNER Phase II. Four test environments were defined, including HST.

[1] "COST" stands for "European Co-operation in the Field of Scientific and Technical Research".

Existing standardized channel models assume that channels are Wide-Sense Stationary Uncorrelated Scattering (WSSUS) [19], which is not satisfied in the HST environment [20]. Furthermore, HST channel models differ significantly from those available for other mobile cellular systems [19], [21]: i) **Different scenarios and propagation conditions must be considered**: communication channel environment is highly variable (e.g. viaducts, hilly terrain or tunnels). ii) **Line of Sight (LoS) conditions dominance**: current HST routes and network plans ensure LoS in most of the cases, thus multipath looses significance. iii) **Doppler Frequency relevance**: due to the high-speed condition, the Doppler-spread magnitude can become high for any carrier frequency, varying rapidly when the train approaches a base station as the angle between transmit-receive antennas and the trackside changes rapidly.

Due to the variability of the scenarios mentioned, it is difficult that *traditional* models can reliably characterize general HST propagation conditions. Therefore, measurement campaigns are necessary for modeling the propagation condition. Although most of the studies are solely based on simulations dealing with HST channel modeling (e.g. [22], [23]), several results based on empirically obtained data can be found. For example, a propagation path-loss model is proposed for high-speeds in viaduct and plain scenarios [24]. In order to tune free-space path-loss models to fit those scenarios, a measurement campaign was performed on a passenger-dedicated line employing a commercially-available network. The maximum reached speed was $340$ km/h, while the bandwidth was limited to $200$ kHz (between $930.2$ and $933.4$ MHz). The downlink receiver is based on a Griffin receiver [25], a Global Positioning System (GPS), a computer, a single receive antenna placed on the rooftop of the train, and processing software. No more details about the measurement setup were provided. The performance of LTE for the HST environment is also assessed in [26] considering a hybrid HST channel model in 3GPP and large-scale models based on the aforementioned measurement campaigns. The resulting channel model consists of a Winner II model for supplying multipath fading [16], HST channel model as defined in 3GPP for providing the Doppler shift profile [27], and large-scale models based on the measurement campaign.

Channel measurements were also obtained by using Elektrobit PropSound multidimensional radio channel sounder [28] as well as the Rohde&Schwarz TSMQ radio network analyzer on the High Speed Integrated Inspection Train (NHSIIT) in China, using GPS receivers for synchronization purposes. Recorded acquired signals were processed for obtaining small-scale and large-scale channel characteristics. Different HST scenarios were considered.

An efficient channel sounding method using cellular communication systems is proposed for the HST environment in [21]. Using Wideband Code Division Multiple Access (WCDMA) signals, a measurement campaign was conducted in real-world HST scenarios. Two different receivers were considered: The Rohde&Schwarz TSMQ Radio Network Analyzer and a custom wireless channel data recorder. The first one is highly convenient because it is portable while implementing most of the tasks of a practical receiver (e.g. cell search and synchronization). Unfortunately, as included algorithms are proprietary, users cannot modify them according to their interests. The custom receiver is more flexible. It comprises the main stages of Intermediate Frequency (IF) sampling followed by digital down-conversion and filtering, all performed in the Field Programmable Gate Array (FPGA). Acquired signals are transmitted via Peripheral Component Interconnect Express (PCIe) to a workstation to be recorded in a Solid-State Drive (SSD). Synchronization between transmitter and receiver nodes is implemented by means of the GPS timing signal.

## III. Requirements for HST Measurements

In the introduction we have stressed the necessity of carrying out measurement campaigns in HST scenarios for modeling the wireless channel and testing the feasibility of LTE, providing insightful data to deploy optimized LTE networks in such scenarios. From now on, we point out the main requirements found for measurement campaigns in HST environments.

### *A. Hardware Requirements*

HST environments demand for very specific measurement hardware features:

**Small and light**. The space available in train cars used to be limited. Additionally, although track sides are spacious, specific places in which the installation of additional hardware is allowed are very limited. This is mainly due to safety reasons, to not interfere with existing systems, and to avoid disturbing routine maintenance procedures. Consequently, hardware size is an important restriction. Additionally, it is very convenient that all hardware can be installed in racks, thus easing its installation and transportation.

**Low-power consumption**. At the time of designing and building the testbed for measuring in HST one does not know if electricity is readily available, which is especially true for base station equipment at the track sides. Therefore, measurement hardware must be easy to power from different sources (e.g. batteries). Additionally, those devices that need to be powered for long-time periods (e.g. rubidium oscillators or GPS receivers) require bulky Uninterruptible Power Supply (UPS) units, impacting on the equipment size and weight.

**Robustness**. HST measurement environments are very harsh and hostile. Complications come from poor working conditions (e.g. absence of light, coldness, and dust). Therefore, hardware connections and internal mountings must be robust; all ports and connectors must be correctly labeled; and software tests are required to validate the hardware setup. Additionally, it is also convenient to test the installation procedures beforehand.

**Frequency agile**. There is no agreement about the spectrum bands assigned to LTE for railway systems. Therefore, multi-band agile Radio Frequency (RF) hardware is required for covering frequencies ranging from $400$ MHz to $6$ GHz.

**Scalability** Although there is a lot of potential knowledge to be gathered from single-antenna measurements, current wireless communication standards –being LTE an example– employ MIMO techniques. To this end, both hardware and software involved in the measurement devices should scale from point-to-point single-antenna to multi-user and multiple-antenna employing several base stations.

**Time and frequency synchronization**. Movement of the transmitter, receiver or scatterers generate Doppler shifts.

Being able to measure such Doppler effects requires near-perfectly frequency-synchronized transmitter-receiver pairs. A well known solution towards this end consists in employing GPS-disciplined oscillators providing frequency and time references which are further stabilized by means of Rubidium oscillators, specially convenient when measuring in areas wihtout GPS coverage (e.g. tunnels).

**Automatic Gain Control (AGC)**. AGC is a feature found in almost all wireless receivers. However, when measuring the performance of such receivers, the AGC is a source of disturbances since the properties of the receiver are modified when the gain changes (e.g. noise figure or non-linearities). Unfortunately, high-speed measurements demand for an enormous dynamic range, which is a problem to be tackled by the measurement hardware (e.g. including a custom AGC based on Received Signal Strength Indication (RSSI) values) or by the measurement methodology (e.g. consistently employing several transmit power values).

**Persistence of acquired data**. Although carrying out measurements employing real-time prototypes has many benefits, the unknown of fundamental design parameters (e.g. path loss) makes such an option very prone to fail because a single mistake in the receiver design or implementation can ruin a measurement campaign completely. The utilization of commercial devices (e.g. channel sounders) is a possible choice, but lacking customization and making the measurements harder to reproduce. Therefore, a convenient technique consists in persistently saving all acquired signals for later off-line evaluation. Now the challenge is to deal with the enormous sampling rates required (note that more than 5.7 GB of raw data are produced per minute when our testbed operates at the maximum data rate achievable) together with harsh measurement conditions (e.g. movement, vibrations). Fortunately, SSD is a mature and affordable technology which also offers storage speeds suitable for this purpose.

**Redundancy and fault tolerance**. Hardware redundancy is required in HST measurements because they are carried out in very short time (usually not more than a couple of days). For example, in a point-to-point measurement, additional receivers can be installed to provide redundancy and diversity in the measurement. On the other hand, sensitive or error-prone components must have spare parts. Examples are power supplies, cables, SSD drives, memory modules, and so on.

**Budget**. The cost of a HST measurement campaign can vary enormously depending on unforeseeable conditions (risk factors). Therefore, measurement hardware has to be designed for minimizing those risk factors. For example, employing affordable hardware makes it easier to scale, to replicate, and to replace in case of malfunctioning. However, notice that the hardware still has to fulfill stringent requirements (e.g. noise figure, linearity) to provide reliable measurements.

**Simplicity**. Typical measurement campaigns in HST scenarios require first to set up all hardware plus the auxiliary infrastructure (e.g. power and coaxial cables and radio masts.) in spaces usually unknown beforehand. Secondly, the measurements are carried out and data is collected. Finally, all installed devices are taken away. The total time window for such a process is very short (sometimes just half a day). The main reason is that such measurements are carried out when there is no ordinary traffic on the rails or during maintenance operations[2]. As an additional drawback, the whole procedure usually takes place during the night; under poor light conditions; in unknown places; at unusual working times; in hostile, harsh, and unfriendly environments[3], etc.

All aforementioned reasons demand for extremely easy-to-use and easy-to-deploy hardware because setup time is very limited. Typically, one arrives at the measurement place with radio masts in which antennas and coaxial cables are already mounted, transmitter and acquiring devices are ready to use immediately after starting up, oscillators are warmed up, etc. We have to maximize the time dedicated to the measurements while guaranteeing their reliability.

### *B. Common Hardware and Software Requirements*

There are some specific requirements impacting simultaneously on measurement software and hardware:

**Traceability**. Knowing all configuration parameters and their evolution during the course of a measurement is fundamental for documenting the results as well as for detecting problems during or after the measurements.

**Autonomy**. Auxiliary connections between measurement nodes are not feasible in HST scenarios. Therefore, all nodes must operate autonomously, being impossible to notify errors during the course of the measurement.

**Verification and Validation**. All hardware and software involved in HST measurements must be carefully verified and validated in order to avoid problems during the measurements.

## IV. TESTBED HARDWARE

Based on the requirements imposed by the HST environment (see Section III), and in our prior experience on building wireless testbeds[4], we have decided to use Ettus [29] Universal Software Radio Peripheral (USRP) N210 [30] as the basis measurement hardware. The USRP hardware from Ettus greatly reduces development costs in terms of hardware as well as manpower. The availability of the USRP N200 series, a low-cost, mid-performance, real-time capable system equipped with a great variety of pluggable RF front-ends covering almost any frequency band from 50 MHz to 2.9 GHz, and from 4.9 GHz to 5.9 GHz leads to a unique device all over the world. Furthermore, such hardware is complemented with the USRP Hardware Driver (UHD) software [31], an open-source, flexible, efficient, and powerful software driver for USRP devices. It is also possible to take advantage of GNU Radio [32], which is a free and open software development kit for Software-Defined Radio (SDR).

[2]If the measurements are limited to collect data from commercially available networks, then it is possible to carry out such measurements during normal train operation.

[3]Measurements disturb railway worker's duties because people from the research team is not used to such harsh environements.

[4]*In order to conduct double-blind revision of the proposed paper, all references from the authors have been omitted. If accepted, the final version of the paper will include such references.*

### A. The USRP N210 Motherboard

The USRP N210 [33] is an affordable piece of hardware including all components necessary for transmit/receive signals from/to a host Personal Computer (PC) to/from the antenna (see top of Fig. 2). Signal samples are exchanged between the host PC and the USRP through a Gigabit Ethernet connection. Real-time interpolation and decimation filters as well as digital mixing are all implemented in the Xilinx Spartan 3A-DSP 3400 FPGA. Digital to Analog Converters (DACs) and Analog to Digital Converters (ADCs) respectively correspond to the Analog Devices AD9777 16-bit dual-DAC [34] and the Texas Instruments ADS62P44 14-bit dual-ADC [35]), both configured to sample at 100 MHz[5].

The USRP N210 is specified to manage up to 50 MHz of bandwidth shared between the transmitter and the receiver sections with full-duplex operation. It also features a single DAC-ADC pair, which leaded to the incorporation of mechanisms for coherently synchronizing several USRP units by incorporating a user-configurable clock distribution system which allows for employing a GPS-disciplined oscillator provided by Ettus under the denomination GPSDO [36]. The USRP also includes a specific multi-antenna expansion port allowing coherent synchronization of two USRP units.

The USRP becomes also an attractive device for rapid prototyping of wireless communication systems since it supports the utilization of the included FPGA as well as attaching a high-performance FPGA by means of a 2.2 Gbit high-speed serializer/deserializer, opening the door for SDR-based, real-time, high-performance, multiple-antenna, broadband wireless communication systems at a low cost. Finally, Ettus declares a Spurious-Free Dynamic Range (SFDR) of 88 dBc for the ADCs and of 80 dBc for the DACs, while frequency accuracy is of 2.5 ppm for the standard TCXO oscillator and up to 0.1 ppm when the GPSDO is employed.

### B. RF Daughter Boards

Ettus provides transceiver daughter boards, being WBX, SBX, RFX900, and XCVR2450 the most attractive for measuring LTE. All transceiver daughter boards are multiple-antenna capable and completely reconfigurable by software. They also incorporate a transmit/receive switch, built in RSSI measurement capability, AGC, adjustable transmit power, and finally, some of them can operate in a full-duplex way.

### C. Testbed Structure

The proposed testbed for LTE measurements in HST scenarios (see Fig. 1) consists of the following hardware components for two transmit/receive half-duplex nodes (see Fig. 2):

**Host**. Each node is based on a PC equipped with robust components for HST environments (e.g. industrial power supply, watertight liquid cooling system, SSDs drives, etc.). In addition to the large storage media requirement (see Section III-A), powerful components are required by the PC so it can handle high data rates and perform some real-time processing tasks (see Section V-A).

[5]The AD9777 also incorporates a four-times interpolation filter in the analog domain.

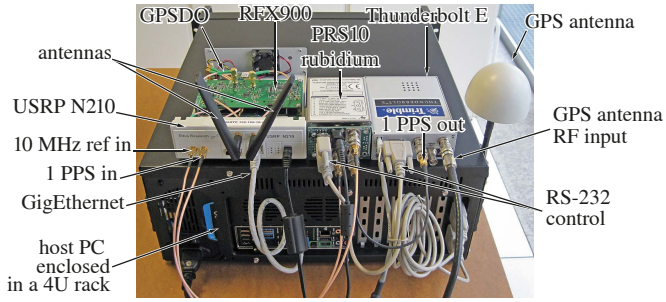


Fig. 1. Picture of a node from the testbed. Notice that all components appear outside the PC case but they perfectly fit inside it (except the antennas).

**Motherboard**. It consists of a USRP N210 connected to the host by means of a dedicated point-to-point Gigabit Ethernet.

**Daughter Board**. We can plug in two different daughterboard sets: The RFX900 covering frequencies from 700 to 1050 MHz, and the XCVR2450, which is a dual-band transceiver covering both Industrial, Scientific and Medical (ISM) bands at 2.4 and 5 GHz.

**Oscillators**. Although the USRP N210 has an internal 10 MHz TCXO reference oscillator which can be updated by the GPSDO, we rely on the Trimble Thunderbolt E GPS [37] plus the SRS PRS10 Rubidium oscilator [38] to provide outstanding stability when GPS coverage is temporary lost.

**Power amplifiers, antennas and filters**. RF daughter boards include internal power amplifiers which can be completed with external ones as for example the Mini-Circuits TVA-11-422). Analogously, internal Low-Noise Amplifiers (LNAs) can also be complemented with external ones (e.g. Mini-Circuits ZHL-2010). Analog filters can also be used to improve signal quality. Finally, we use commercially available antennas.

Our solution is also easily reproducible because we employ hardware available off-the-shelf. The cost of all components for two nodes is about 15 000 EUR, including taxes.

## V. Testbed Software

The hardware described in Section IV-C is complemented with UHD plus a custom-made sophisticated software system comprised by three main parts (see Fig. 2): 1) Low-level and real-time processing software module; 2) Receiver synchronization module; and 3) High-level transmitter/receiver and channel emulation modules. The next sections briefly describe each one of the aforementioned software modules.

### A. Low-level and Real-time Processing Software Module

The low-level and real-time processing software module (see Fig. 2) is in charge of interfacing with the testbed hardware in order to perform control tasks as well as some kind of real-time processing required during the measurement campaigns. All nodes are equipped with a custom-made multi-thread software solution consisting of the following subsystems (see Fig. 3):

**UHD interface subsystem (UHDIS)**. It is based on the UHD driver provided by Ettus together with the Boost C++ Libraries [39]. The UHD converts the USRP in one of the very few hardware pieces of this kind that works out of the box. It comes with lots of examples plus a very complete Application

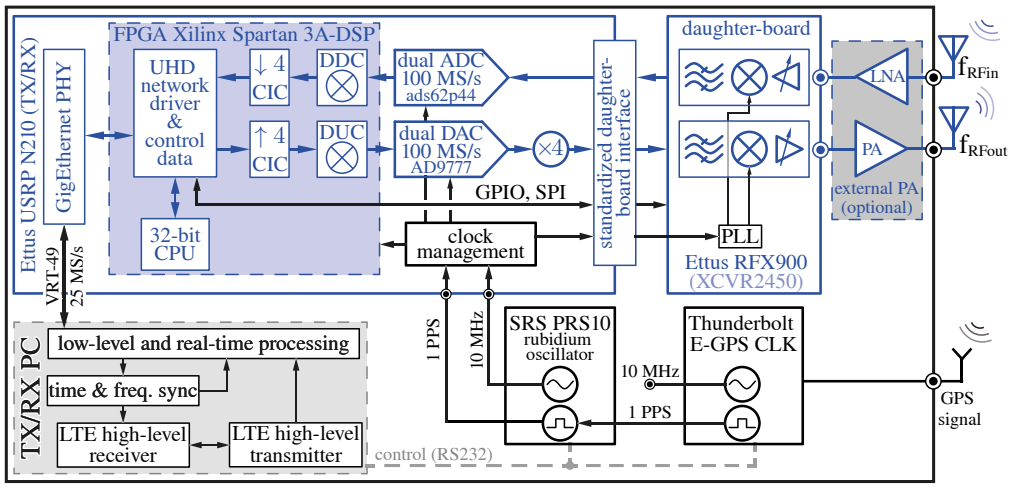


Fig. 2. Scheme of the testbed hardware consisting of a PC, a USRP N210 with the RFX900 RF daughter board and the GPS+Rubidium reference oscillators.

Programming Interface (API) to configure almost all hardware parameters. All Ettus RF daughter boards are also supported.

**Persistence Subsystem (PERS)**. It is responsible for exchanging and re-sampling the signals to be transmitted/acquired between the storage media (SSD drives) and the UHDIS employing the ANSI/VITA VRT 49 format. At the transmitter side, the signals are loaded into the host memory to be later transmitted over the air. At the receiver side, PERS stores the acquired signals at a sampling rate of 25 Msample/s (complex-valued with 16 bits per sample), resulting in a net transfer rate of 100 Mbyte/s. PERS also allows for periodically inspecting the acquired signals by means of the Signal Integrity Subsystem (SIS) to ensure the correct behavior of the receiver. Notice that PERS operates autonomously on a high-priority thread

**Management and Monitoring Subsystem (MAMOS)**. It allows for modifying hardware parameters during the course of a measurement, recording when and what was modified together with monitoring information which is recorded periodically for traceability purposes. A transactional mechanism is implemented. If a modification on the hardware configuration causes an error, the hardware is reverted to the last known configuration (a complete hardware reset might be required). MAMOS exports a command-based API ensuring that all those commands are transactional. Although the direct access to the UHD through UHDIS is possible, the protection

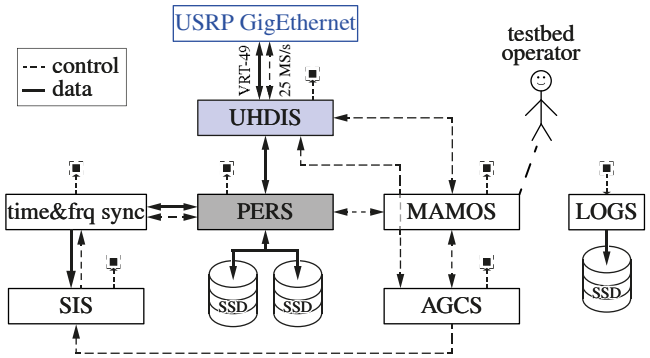


Fig. 3. High-level scheme of the low-level and real-time processing software. Note that all software modules are connected to "LOGS".

provided by MAMOS would disappear. Currently, there are commands for transmitting and acquiring signals, for configuring the RF carrier, and for changing power amplifier gains. MAMOS depends on Log subsystem (LOGS) and PERS. If a problem is detected on the hardware that interrupts the transmission/acquisition of signals, the event is first logged (LOGS) and PERS is notified to invalidate such signals for further evaluation. Additionally, MAMOS implements a simple user interface for the testbed operator which is employed to show alerts of hardware malfunctioning, signal acquisition parameters via SIS, etc.

**AGC subsystem (AGCS)**. As mentioned above, HST measurements could demand for AGC. AGCS can autonomously control and record the receiver gain based on the RSSI values provided by the USRP through UHDIS.

**SIS**. It is not possible to completely evaluate the acquired signals during the course of a measurement. However, in order to avoid fully blind measurements (e.g. not knowing if the acquired data is going to be useful) we have incorporated a subsystem that periodically checks the already-persisted signals to test their integrity. This is done by running the receiver synchronization module in a low-priority thread to not disturb the signal acquisition process. During this process, both Signal-to-Noise Ratio (SNR) and Signal to Interference and Noise Ratio (SINR) rough estimations are also provided and sent to MAMOS to inform the testbed operator. If the synchronization is not successful, MAMOS is notified and the event is logged (LOGS). The testbed operator is also informed.

**LOGS** records all important events created by the subsystems.

The aforementioned subsystems run in parallel at the transmitter/receiver nodes, being responsible for transmitting and acquiring signals while controlling and monitoring the hardware, notifying the testbed operator in case of any problem while, at the same time, informing about the whole process.

Once the measurement campaign has finished, it is necessary to evaluate all acquired data. First, all signals recorded by PERS have to be sorted so that those portions invalidated by problems in the hardware are taken away. This task is done by the PERSReader subsystem, which runs off-line from the data stored by PERS. Subsequent software modules enable to

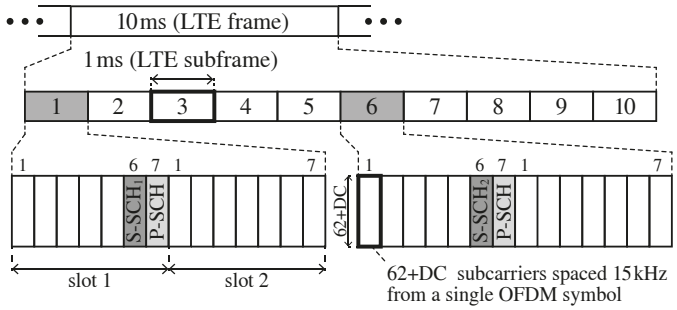


Fig. 4. LTE synchronization signals.

process the signals recorded in order to extract and further evaluate acquired LTE frames.

### B. Receiver Synchronization Module

According to [40], an LTE frame (see Fig. 4) is comprised by 10 subframes of 1 ms of duration while each subframe contains two slots. Each slot is formed by 7 Orthogonal Frequency-Division Multiplexing (OFDM) symbols when normal Cyclic Prefix (CP) length is used (6 symbols for extended CP mode).

The LTE standard defines the Primary Synchronization Signal (P-SCH) and the Secondary Synchronization Signal (S-SCH). These signals allow the User Equipment (UE) to identify the physical layer cell by means of the Physical Cell Identity (PCI). According to [40, Section 6.11], there are $504$ unique PCIs, grouped in $168$ physical-layer cell-identity groups, each group containing three unique identities. The P-SCH, as defined in [40, Section 6.11.1], depends on the index of the PCI within a physical-layer cell-identity group, namely $N_{\text{ID}}^{(2)} \in \{0, 1, 2\}$. Once $N_{\text{ID}}^{(2)}$ is known at the receiver, the detection of the S-SCH will enable to obtain the physical-layer cell-identity group number, namely $N_{\text{ID}}^{(1)} \in \{0, 1, \ldots, 166, 167\}$. For the remaining of the explanation, Frequency-Division Duplex (FDD) transmission mode is assumed as well as normal CP mode, although the synchronization process in other cases is similar.

When FDD transmission mode is considered, P-SCH is transmitted by using the $62$ subcarriers symmetrically arranged around the DC-carrier of the seventh symbol of the first slot of first and sixth subframes of each LTE frame (see Fig. 4). In the same way, S-SCH is transmitted using the same subcarriers of the OFDM symbols preceding those that contain the P-SCH. The S-SCH is interleaved into two half-length sequences, namely First Secondary Synchronization Sequence (S-SCH$_1$) and Second Secondary Synchronization Sequence (S-SCH$_2$), which are transmitted on the first and sixth subframes of each LTE frame, respectively (see Fig. 4).

Time and frequency synchronization modules were implemented in Matlab scripts. Matlab environment was chosen due to its flexibility, efficiency (as operations involved in synchronization tasks, such as correlations, are computationally expensive) and because it can be easily integrated with other software modules. The latter aspect is relevant because the synchronization runs in parallel with SIS and PERS.

On the one hand, the time synchronization process comprises (a) slot-level, and (b) frame-level synchronization. In the first one, the starting time of each slot is encountered. On the second part, each half-frame is marked as the first or the second one of an LTE frame.

In order to achieve slot-level synchronization, the three different P-SCHs are searched along the received signal. In order to do this, the received signal is divided into blocks whose length equals that of an LTE half-frame (i.e. $5$ LTE subframes). For each block, the correlation with the three possible P-SCH signals is performed and the result is added together with those from a configurable number of the previous blocks. Then, the initial sample of each slot is detected by looking for the correlation maximum values. $N_{\text{ID}}^{(2)}$ is also obtained. The summation operation enables to compensate for eventual misdetections, being the process adaptive and so it can handle variable delays. Once the base station $N_{\text{ID}}^{(2)}$ is known, then the computational complexity can be reduced as only a single P-SCH sequence must be considered.

Once the signal is synchronized at slot level, the synchronization at frame-level can be performed. Note that the previously detected P-SCH is used as a reference to perform channel estimation and de-scramble the S-SCH. In this case, all the processing is performed in the frequency domain, so firstly the CP of each OFDM symbol is discarded. After the Fast Fourier Transform (FFT), the $62$ subcarriers symmetrically arranged around the DC-carrier of the sixth OFDM symbol of the first slot of the first and sixth subframes of each LTE frame are extracted. Due to the difference between the synchronization signal transmitted in the first and sixth subframes, synchronization at frame-level can be achieved. In order to do this, the correlation with four sequences defining the S-SCH (see [40, Section 6.11.2.1]) is obtained for each extracted symbol. In order to jointly detect the S-SCH$_1$ and the S-SCH$_2$, correlation results for each two consecutive extracted symbols are combined (multiplied). As in the previous case, the results for a fixed number of consecutive symbols are summed together to compensate for eventual misdetections. Finally, the peaks of the correlations enable for distinguishing between the first and second half-frames of each LTE frame. Note that, if no a priori information is provided, the correlations must be obtained for each of the possible $N_{\text{ID}}^{(2)}$ values. Once $N_{\text{ID}}^{(2)}$ is known beforehand, the process becomes much less computationally complex.

Frequency synchronization is performed in two steps: 1) Fractional Frequency Offset (FFO) compensation, and 2) Integer Frequency Offset (IFO) compensation. While the second one compensates the part of the frequency offset which is multiple of the subcarrier spacing, the first one compensates the rest. The first compensation is made by taking advantage of the CP of each OFDM symbol. In order to do this, a Maximum Likelihood (ML) method derived in [41] (see also [42]) was implemented. On the other hand, the IFO compensation is performed in the frequency domain. With the aim of making the IFO compensation scheme independent from the transmitter parameters, only the S-SCH is used. The compensation is based on the ML method proposed in [41].

### C. LTE High-level Transmitter and Receiver Modules

A model of the transmitter, receiver, and configurable wireless channel was developed using the Synopsys SPW [43] software and the Synopsys SPW LTE/LTE-A Library [44].

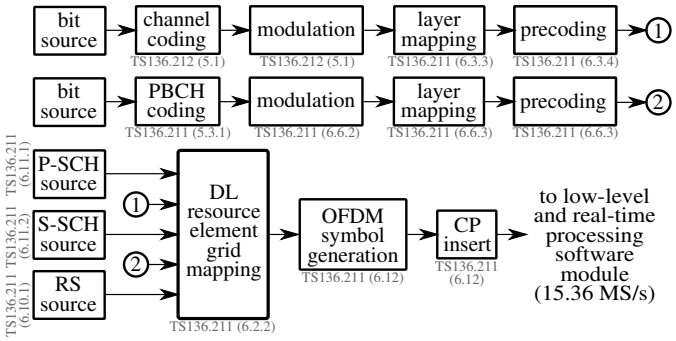


Fig. 5. Scheme of the implemented transmitter software module.

The whole physical layer of LTE is implemented. At the transmitter side (see Fig. 5), first the bits to be transmitted are generated and the channel coding procedure described in [45, Section 5.] is applied. Encoded bits are mapped into complex-valued constellation points and grouped into LTE codewords. Then, these codewords are mapped into layers according to [40, Section 6.3.3]. After that, precoding according to [40, Section 6.3.4] is applied. On the other hand, P-SCH and S-SCH are generated together with random bits simulating the Physical Broadcast Channel (PBCH) contents. These bits are convolutionally encoded according to [45, Section 5.3.1], grouped into codewords, scrambled, modulated, and precoded. Also reference signals are generated in accordance to [40, Section 6.10.1]. Contents of downlink resource element grid are generated by combining the precoded data, PBCH contents, reference signals, and synchronization as defined in [40]. The results are then mapped into OFDM symbols and the CP is inserted for each of them.

At the receiver side (see Fig. 6), the CP of each OFDM symbol is discarded and the subcarrier contents are extracted by means of the FFT operation. Channel estimation and equalization is then performed. Next, data symbols in the downlink resource element grid are extracted together with the reference and synchronization symbols. Data from control channels such as Physical Downlink Control Channel (PDCCH), Physical Control Format Indicator Channel (PCFICH), Physical Hybrid-ARQ Indicator Channel (PHICH) as well as user data contained in the Physical Downlink Shared Channel (PDSCH) and the contents of the PBCH are also gathered. The data received on PBCH is layer-demapped, demodulated, and descrambled, then convolutionally encoded codewords will be decoded into PBCH bits as described in [45, Section 5.3.1] and the Cyclic Redundancy Code (CRC) will be checked. Similar steps are performed on the data received on PDCCH, and the Downlink Control Information (DCI) bits are extracted as described in [45, Section 5.3.3]. Similarly, symbols received on PCFICH are layer-demapped, demodulated, de-scrambled, and decoded to obtain a Control Format Indicator (CFI) value per received subframe according to [45, Section 5.3.4.1]. Also, the symbols received in PHICH are layer-demapped, despreaded, descrambled, and decoded in order to obtain an HARQ Indicator (HI) value associated with a single user. Concerning the data received on the PDSCH, symbols are first layer-demapped and demodulated for obtaining soft-bit decisions. Then, channel decoding according to [45, Section 5.1] is performed, which implies tasks such as descrambling, deinterleaving, combination with previous transmissions (e.g. for Hybrid Automatic Repeat Request (HARQ) processing) and turbo-

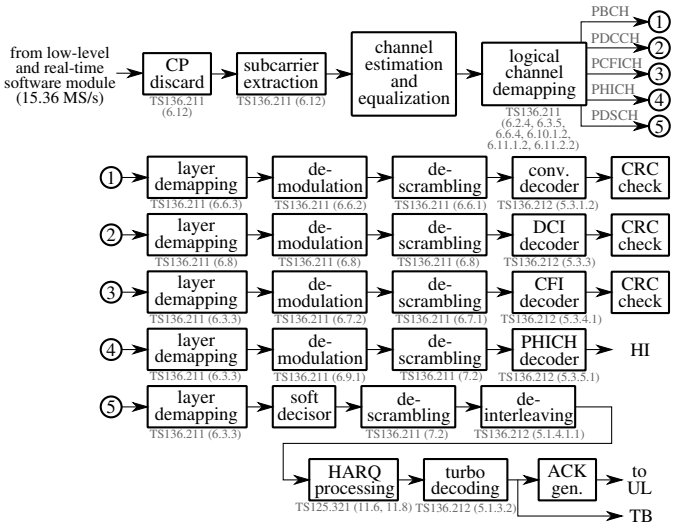


Fig. 6. Scheme of the implemented receiver software module.

decoding. Transport Blocks (TBs) are extracted and their CRCs are checked in order to generate Positive-Acknowledgement (ACK) or Negative-Acknowledgement (NACK) responses.

The previously described transmitter and receiver models can be connected through a MIMO channel model and simulations can be performed in order to compare the results provided by different channel models to those obtained experimentally. HST propagation condition according to the model described in [46, Annex B.3] is supported by such a MIMO channel model.

Both the synchronization modules as well as the transmitter, receiver, and channel emulation ones support FDD and Time-Division Duplex (TDD) transmission modes. Furthermore, they are highly-configurable and enable to modify most of the parameters defining the LTE transmission scheme, such as the number of transmitter and receiver antennas, number of subcarriers, modulation type, and so on. This enables not only flexibility for simulation purposes, but also for scaling the proposed architecture to MIMO schemes. It is worth noting that, compared to most commercial solutions, all processing blocks can be customized, thus allowing for defining and testing new algorithms.

## VI. Conclusions and Future Work

A flexible, easily scalable, and cost-affordable hardware and software architecture was proposed for measuring –and later evaluating– LTE in HST scenarios. HST environments have been found to have very different characteristics from those of typical mobile cellular environments. This has two main implications: 1) Most of the available channel models are not accurate enough and thus measurement campaigns are required to improve them; 2) Severe requirements are imposed on testbed hardware and software as well as measurement procedures.

The main future lines to conduct our research are first, to evaluate the performance of the proposed testbed architecture on real-world HST environments. Secondly, to extend the proposed testbed architecture in order to achieve full real-time operation. A possibility could be to perform most of the software processing tasks on FPGAs [47], [48]. Finally, the

performance of time and frequency synchronization algorithms can be improved for the HST environment. In order to do so, custom-made channel emulators are very convenient prior to real-world measurements.

## ACKNOWLEDGMENTS

This work has been funded by Xunta de Galicia, MINECO of Spain, and FEDER funds of the EU under grants 10TIC003CT, 2012/287, IPT-2011-1034-370000, TEC2010-19545-C04-01, CSD2008-00010, and FPU12/04139.

## REFERENCES

[1] S. Sesia, I. Toufik, and M. Baker, Eds., LTE The UMTS Long Term Evolution from theory to practice, 2nd ed. John Wiley & Sons, 2011.

[2] European Commision, "Digital Land Mobile Radio Communications-COST 207 Final Report," 1989.

[3] European Commision, "Digital Mobile Radio towards Future Generation Systems-COST 231 Final Report," 1993.

[4] European Commision, "Wireless Flexible Personalised Communications-COST 259 Final Report," 2001.

[5] European Commision, "Towards Mobile Broadband Multimedia Communications-COST 273 Final Report," 2006.

[6] W. Braun and U. Dersch, "A physical mobile radio channel model," *IEEE Transactions on Vehicular Technology*, vol. 40, no. 2, pp. 472 –482, may 1991, doi: 10.1109/25.289429.

[7] D. Cygan, F. David, H. Eul, J. Hofmann, N. Metzner, and W. Mohr, "RACE-II advanced TDMA mobile access project An approach for UMTS," in *Mobile Communications Advanced Systems and Components*, ser. Lecture Notes in Computer Science, C. Günther, Ed. Springer Berlin / Heidelberg, 1994, vol. 783, pp. 428–439.

[8] ITU-R, "Guidelines for evaluation of radio transmission technologies for IMT-2000. ITU-R Recommendation M.1225," 1997.

[9] ETSI, "ETSI TS 125 101: UMTS; User Equipment (UE) radio transmission and reception (FDD)."

[10] Siemens, "High speed environment channel models (R4-050388)," May 2005, 3GPP TSG-RAN Working Group 4 (Radio) meeting #35.

[11] Ericsson, Nokia, Motorola, and R. . Schwarz, "Proposal for LTE channel models (r4-070572)," 2007, 3GPP TSG-RAN Working Group 4 (Radio) meeting #43.

[12] ETSI, "ETSI TS 136 141: LTE; E-UTRA; Base Station (BS) conformance testing."

[13] ETSI, "ETSI TR 125 996: UMTS; Spacial channel model for MIMO simulations."

[14] D. Baum, J. Hansen, and J. Salo, "An interim channel model for beyond-3G systems: extending the 3GPP spatial channel model (SCM)," in *2005 IEEE 61st Vehicular Technology Conference, 2005. VTC 2005-Spring.*, vol. 5, pp. 3132 – 3136 Vol. 5, may-1 june 2005, doi: 10.1109/VETECS.2005.1543924.

[15] Ericsson, Elektrobit, Nokia, Motorola, and Siemens, "LTE Channel models and simulations (R4-060334)," February 2006, 3GPP TSG-RAN Working Group 4 (Radio) meeting #38.

[16] P. Kyosti, J. Meinila, L. Hentila, X. Zhao, T. Jamsa, C. Schneider, M. Narandzic, M. Milojevic, A. Hong, J. Ylitalo, V.-M. Holappa, M. Alatossava, R. Bultitude, Y. de Jong, and T. Rautiainen, "IST-4-027756 WINNER II D1.1.2 V1.1: WINNER II Channel Models," July 2007.

[17] ITU-R, "Guidelines for evaluation of radio interface technologies for imt-advanced, Report ITU-R M.2135-1," December 2009.

[18] 3GPP, "3GPP TR 36.814: 3GPP;Technical specification group radio access network; E-UTRA; Further advancements for E-UTRA physical layer aspects," Tech. Rep.

[19] T. Zhou, T. Cheng, L. Liu, Q. Jiahui, and S. Rongchen, "High-speed railway channel measurements and characterizations: a review," *Journal of Modern Transportation*, vol. 20, no. 4, pp. 199–205, 2012.

[20] A. Ghazal, C.-X. Wang, H. Haas, M. Beach, X. Lu, D. Yuan, and X. Ge, "A non-stationary mimo channel model for high-speed train communication systems," in *2012 IEEE 75th Vehicular Technology Conference (VTC Spring)*, pp. 1–5. IEEE, 2012.

[21] L. Liu, C. Tao, T. Zhou, Y. Zhao, X. Yin, and H. Chen, "A highly efficient channel sounding method based on cellular communications for high-speed railway scenarios," *EURASIP Journal on Wireless Communications and Networking*, vol. 2012, no. 1, pp. 1–16, 2012.

[22] Y. R. Zheng and C. Xiao, "Simulation models with correct statistical properties for Rayleigh fading channels," *IEEE Transactions on Communications*, vol. 51, no. 6, pp. 920 – 928, june 2003, doi: 10.1109/TCOMM.2003.813259.

[23] C. Xiao, Y. R. Zheng, and N. Beaulieu, "Novel Sum-of-Sinusoids Simulation Models for Rayleigh and Rician Fading Channels," *IEEE Transactions on Wireless Communications*, vol. 5, no. 12, pp. 3667 – 3679, december 2006, doi: 10.1109/TWC.2006.256990.

[24] H. Wei, Z. Zhong, K. Guan, and B. Ai, "Path loss models in viaduct and plain scenarios of the high-speed railway," in *2010 5th International ICST Conference on Communications and Networking in China (CHINACOM)*, pp. 1 –5, aug. 2010.

[25] Aeroflex GmbH, "8300 Series Griffin – Fast Measurement Receiver – User's guide," 2011.

[26] K. Guan, Z. Zhong, and B. Ai, "Assessment of LTE-R Using High Speed Railway Channel Model," in *2011 Third International Conference on Communications and Mobile Computing (CMC)*, pp. 461 –464, april 2011, doi: 10.1109/CMC.2011.34.

[27] ETSI, "ETSI TS 136 104: LTE; E-UTRA; Base Station (BS) radio transmission and reception."

[28] Elektrobit, "PropSoundTM CS Multi-Dimensional Channel Sounder General presentation, Finland," 2005.

[29] "Ettus Research LLC." http://www.ettus.com

[30] "USRP N210." https://www.ettus.com/product/details/UN210-KIT

[31] "USRP Hardware Driver (UHD)." http://ettus-apps.sourcerepo.com/redmine/ettus/projects/uhd/wiki

[32] "GNU Radio." http://gnuradio.org/

[33] "Ettus USRP N210." https://www.ettus.com/content/files/07495_Ettus_N200-210_DS_Flyer_HR_% 1.pdf

[34] "Analog Devices AD9777." http://www.analog.com/static/imported-files/data_sheets/AD9777.pdf

[35] "Texas Instruments ADS62P44." http://www.ti.com/lit/gpn/ads62p44

[36] "Ettus GPSDO." https://www.ettus.com/content/files/gpsdo-kit_4.pdf

[37] "Trimble Thunderbolt E GPS." http://www.trimble.com/timing/thunderbolt-e.aspx

[38] "Standford Research Systems PRS10." http://www.thinksrs.com/products/PRS10.htm

[39] "Boost C++ Libraries." http://www.boost.org/

[40] ETSI, "ETSI TS 136 211: LTE; E-UTRA; Physical channel and modulation."

[41] Q. Wang, C. Mehlführer, and M.-u. Rupp, "Carrier frequency synchronization in the downlink of 3GPP LTE," in *Proceeding of the PIMRC'10, Istanbul, Turkey*, 2010.

[42] S. Caban, C. Mehlführer, M. Rupp, and M. Wrulich, Evaluation of HSDPA and LTE: From testbed measurements to system level performance, 2012.

[43] Synopsys, Inc., "Synopsys SPW: Datasheet," 2011.

[44] Synopsys, Inc., "LTE/LTE-A Library: Datasheet," 2011.

[45] ETSI, "ETSI TS 136 212: LTE; E-UTRA; Multiplexing and channel coding."

[46] ETSI, "ETSI TS 136 101: LTE; E-UTRA; User Equipment (UE) radio transmission and reception."

[47] George Fredric Eichinger III, "CRUSH: Cognitive Radio Universal Software Hardware," 2012.

[48] G. Eichinger, K. Chowdhury, and M. Leeser, "Cognitive radio universal software hardware," in *Dynamic Spectrum Access Networks (DYSPAN), 2012 IEEE International Symposium on*, pp. 270–271. IEEE, 2012.